Effect of Altitude Concentration Gradient of Soluble Gaseous Pollutants on Their Scavenging by Falling Rain Droplets

TOV ELPERIN, ANDREW FOMINYKH, AND BORIS KRASOVITOV

Department of Mechanical Engineering, The Pearlstone Center for Aeronautical Engineering Studies, Ben-Gurion University of the Negev, Beer-Sheva, Israel

(Manuscript received 11 August 2008, in final form 16 January 2009)

ABSTRACT

This paper analyzes absorption of soluble atmospheric trace gases by falling rain droplets with internal circulation, which is caused by interfacial shear stresses. It is assumed that the concentration of soluble trace gases in the atmosphere varies in a vertical direction. In the analysis the accumulation of the absorbate in the bulk of the falling rain droplet was accounted for. The problem is solved in the approximation of a thin concentration boundary layer in the droplet and in the surrounding air. It was assumed that the bulk of a droplet, beyond the diffusion boundary layer, is completely mixed and that concentration of the absorbate is homogeneous and time dependent in the bulk. By combining the generalized similarity transformation method with Duhamel's theorem, the system of transient conjugate equations of convective diffusion for absorbate transport in liquid and gaseous phases with time-dependent boundary conditions is reduced to a linear-convolution Volterra integral equation of the second kind, which is solved numerically. It is shown that the nonuniform vertical distribution of absorbate in a gaseous phase strongly affects mass transfer during gas absorption by a falling droplet.

1. Introduction

Gas absorption by falling rain droplets is of relevance in meteorology and environmental engineering. Rain plays an important role in wet removal of gaseous pollutants from the atmosphere. Scavenging of atmospheric gaseous pollutants by rain droplets is a result of a gas absorption mechanism (Pruppacher and Klett 1997). Comprehensive study of mass transfer during gas absorption by falling rain droplets is a necessary step for adequate predicting of the atmospheric changes under the influence of hazardous gases.

Concentration measurements of CO_2, SO_2, NH_3, and other trace gases in the atmospheric boundary layer revealed vertical (altitudinal) dependence of the concentrations (see Georgii 1978; Gravenhorst et al. 1978; Pérez-Landa et al. 2007; Georgii and Müller 1974; Schulz et al. 2004). The concentration of gases that are not associated with photosynthesis (e.g., SO_2 and NH_3) has a maximum at the earth's surface and decreases with height over the continents. The concentration of NH_3 over the continents decreases rapidly with altitude, reaching a constant background concentration in winter and warm days at altitudes of about 1500 and 3000 m above the ground, respectively (see Georgii and Müller 1974; Georgii 1978). On warm days the ground concentration of NH_3 is considerably higher than on cold days. Sulfur dioxide concentration in the atmospheric boundary layer (ABL) is higher during winter than during summer because of the higher anthropogenic SO_2 production. In contrast to the concentrations of SO_2 and NH_3 over the continents, the profiles of concentration of these gases over the ocean have minima at the ocean surface. This phenomenon is explained by the high solubility of SO_2 and NH_3 in seawater, whereby the ocean acts as a sink of soluble gases (see Georgii and Müller 1974; Georgii 1978). Diurnal and seasonal variations of CO_2 distribution with altitude occur because of the competition between different phenomena, such as photosynthesis, respiration, and thermally driven buoyant mixing (see Denning et al. 1995; de Arellano et al. 2004; Chen et al. 2004, 2005, 2008). During the growing season over the continents, the concentration of CO_2 early in the morning at the ground is very high and sometimes reaches a value of 400 ppmv because of

Corresponding author address: Tov Elperin, Department of Mechanical Engineering, Ben-Gurion University of the Negev, P.O. Box 653, Beer-Sheva 84105, Israel.
E-mail: elperin@bgu.ac.il

DOI: 10.1175/2009JAS2922.1

the nocturnal CO_2 release by soil microbes and other biota. Concentration of CO_2 before the sunrise has a pronounced maximum at the surface and rapidly decreases with height; the magnitude of the gradients of concentration is on the order of 10 ppmv km^{-1}. When the sun rises, the concentration of carbon dioxide at the surface decreases because the uptake of CO_2 due to photosynthesis exceeds the release of CO_2 due to respiration. Note that photosynthesis and thermally driven buoyant convection in the atmosphere are driven by solar radiation and have the same diurnal frequencies (see Denning et al. 1995). Photosynthesis and vertical mixing by convection act to decrease CO_2 in the lowermost part of the CO_2 profile. Joint influence of these two mechanisms results in the vertical distribution of CO_2 with the minimum at the ground and an increase of concentration with height. The minimum of CO_2 concentration at the ground is most pronounced in the afternoon (see Chen et al. 2004). The uptake of carbon dioxide due to photosynthesis slowly decreases in the evening and ceases approximately at the sunset. Correspondingly, from the afternoon to the sunset, the distribution of CO_2 concentration undergoes a change from increasing with height to decreasing with height (see Schulz et al. 2004). After sunset the surface uptake of CO_2 by vegetation ceases, and soil/plant respiration once again enriches the surface layer with CO_2. The CO_2 concentration near the ground steadily increases from the sunset until the next sunrise. The fluxes of CO_2 due to photosynthesis and respiration are one order of magnitude larger than the fluxes resulting from the anthropogenic emissions. During the dormant season, the release of CO_2 due to respiration exceeds the uptake of CO_2 due to photosynthesis, and vertical mixing by convection weakens. These processes produce a profile with a higher CO_2 concentration at the surface and lower concentration aloft over the land. The distribution of concentration with the minimum of CO_2 at the ground is impossible during the dormant season.

Information about the evolution of the vertical CO_2 profile with time allows us to calculate CO_2 fluxes in the ABL. Vertical transport of CO_2 in the ABL is an integral part of atmospheric CO_2 transport and is important for understanding the global CO_2 distribution pattern. An improved understanding of the CO_2 cycle is also essential for the analysis of global climate change. Clouds and rain play an essential role in vertical redistribution of CO_2 and other soluble gases in the atmosphere. Scavenging of soluble gases (e.g., SO_2, NH_3, and CO_2) by rains and clouds contributes to the evolution of vertical distribution of these gases. At the same time, the existence of vertical gradients of soluble gases in the atmosphere affects the rate of gas absorption by rain droplets. Note that the existing models of global transport in the atmosphere (see, e.g., Chen et al. 2004; de Arellano et al. 2004) do not take into account the influence of rain on the biogeochemical cycles of different gases.

Because of differences in the solubility of gases in liquids, mass transfer during absorption of soluble gas by droplets in the presence of an inert admixture can be continuous-phase controlled, liquid-phase controlled, or conjugate. Continuous-phase-controlled mass transfer by falling droplets was discussed by Kaji et al. (1985), Altwicker and Lindhjem (1988), Waltrop et al. (1991), and Saboni and Alexandrova (2001). Liquid-phase-controlled mass transfer was studied by Amokrane and Caussade (1999) and Chen (2001), among others. Mass transfer controlled by both phases was analyzed by Walcek and Pruppacher (1984), Alexandrova et al. (2004), Chen (2004), Elperin and Fominykh (2005), and Elperin et al. (2007, 2008).

The accumulation of the dissolved atmospheric gases in a falling water droplet during absorption—taking into account the vertical distribution of the absorbate concentration in a gaseous phase and the circulation of liquid inside a droplet caused by shear stresses at the interface—can be determined by solving a conjugate problem of unsteady convective diffusion with time-dependent boundary conditions. Analytical solution of this problem requires the application of sophisticated methods in the theory of heat and mass transfer (see, e.g., Bartels and Churchill 1942; Ruckenstein 1967). In all previous studies, mass transfer during gas absorption by falling liquid droplets was investigated for the homogeneous distribution of absorbate in a gaseous phase. In this study we investigate the influence of the absorbate inhomogeneity in a vertical direction in a gaseous phase on the rate of gas absorption by falling droplets. The suggested approach includes application of the generalized similarity transformation to a system of transient equations of convective diffusion and Duhamel's theorem. The problem is reduced to a numerical solution of a linear-convolution Volterra integral equation of the second kind.

2. Description of the model

Consider absorption of a soluble gas from a mixture containing an inert gas by a moving droplet. At time $t = 0$ the droplet begins to absorb gas from the atmosphere. Distribution of the concentration of the absorbate in the gaseous phase in the vertical direction is assumed to be known (see Fig. 1).

In the analysis we account for the resistance to mass transfer in both phases and use the following simplifying assumptions.

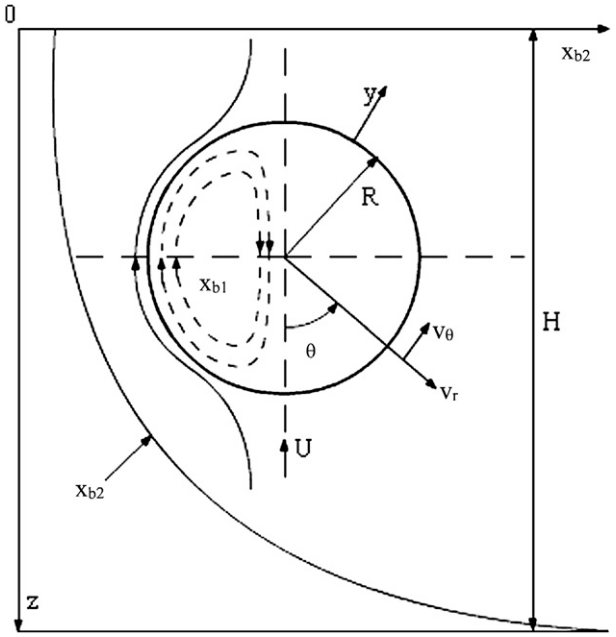

FIG. 1. Schematic view of a falling droplet.

1) We employ the approximation of the infinite dilution of the absorbate in the absorbent.
2) Thermodynamic parameters of the system are assumed constant.
3) Thicknesses of the diffusion boundary layers in both phases are assumed to be small compared with the droplet's size.
4) The tangential molecular mass transfer rate along the surface of a spherical droplet is assumed to be small compared with a molecular mass transfer rates in the normal direction.
5) The bulk of a droplet, beyond the diffusion boundary layer, is assumed to be completely mixed, and the concentration of absorbate is homogeneous in the bulk.
6) The droplet has a spherical shape.
7) The internal circulation inside the droplet and the gas velocity in the vicinity of the droplet have axial symmetry; that is, convective diffusion is determined only by the radial and tangential components of the velocity.

The assumptions about the circulation inside a droplet and the assumption that the droplet has a spherical shape are valid in the following ranges of the falling-in-air water droplet radii, Reynolds numbers, and velocities: $0.1\,\text{mm} \le R \le 0.5\,\text{mm}$, $10 \le \text{Re} \le 300$, and $0.7 \le U \le 4.5\ \text{m s}^{-1}$. Effects of turbulent diffusion and turbulent flow in the air must be taken into account for droplets with $R > 0.8$ mm (see, e.g., Amokrane and Caussade 1999), and they are neglected in the present study. Analysis of fluid flow around a moving droplet shows that at different Reynolds numbers the tangential fluid velocity component in the vicinity of a gas–liquid interface can be approximated by the following equation (see, e.g., Pruppacher and Klett 1997, p. 392):

$$v_\theta = -kU\sin\theta, \tag{1}$$

where the coefficient k is equal to 0.04 in the range of the external flow Reynolds numbers ($\text{Re} = 2UR\rho_2/\mu_2$) from 10 to 300 (see, e.g., Pruppacher and Klett 1997, p. 386). The dependence of the terminal fall velocity of liquid droplets on their diameter was analyzed by Pruppacher and Klett (see Pruppacher and Klett 1997, chapter 10). Following the approach suggested by Ruckenstein (1967), we arrive at the following system of transient equations of convective diffusion for the liquid and gaseous phases, which account for convection in the radial and tangential directions:

$$\frac{\partial X_i}{\partial \tau_i} + \text{Pe}_i\left(-\sin\theta\frac{\partial X_i}{\partial \theta} + 2Y\cos\theta\frac{\partial X_i}{\partial Y}\right) = \frac{\partial^2 X_i}{\partial Y^2}, \tag{2}$$

where $i = 1, 2$; and Pe is the Peclet number ($\text{Pe}_i = kRU/D_i$). The radial fluid velocity component in Eq. (2) is determined by Eq. (1) and by the continuity equation: $v_r = 2k\cos\theta Uy/R$. Equation (2) is written in a frame attached to the falling droplet and is valid for $y \ll R$. Because the velocity of the droplet fall is known and $z = Ut$, the vertical coordinate–dependent boundary conditions can be transformed into the time-dependent boundary conditions. The vertical coordinate z is aligned with the direction of the droplet fall. The initial and boundary conditions for Eq. (2) are

$$X_2 = X_{b2}(\tau_2) \quad \text{as} \quad Y \to \infty, \tag{3}$$

$$X_1 = X_{b1}(\tau_1) \quad \text{as} \quad Y \to -\infty, \tag{4}$$

$$X_1 = mX_2 \quad \text{at} \quad Y = 0, \tag{5}$$

$$N_1 = N_2 \quad \text{at} \quad Y = 0, \tag{6}$$

where $N_i = -D_iC_i\partial x_i/\partial y$; $X_{b1}(\tau_1) = [x_{b1}(t) - mx_{b20}]/(x_{b10} - mx_{b20})$; $X_{b2}(\tau_2) = [x_{b2}(t) - x_{b20}]/(x_{b10} - mx_{b20})$; $y = r - R$, where $y \ll R$; $X_1 = (x_1 - mx_{b20})/(x_{b10} - mx_{b20})$; $X_2 = (x_2 - x_{b20})/(x_{b10} - mx_{b20})$; $\text{Pe}_i = RkU/D_i$; $Y = y/R$; and $\tau_i = tD_i/R^2$. The coefficient $m = HR_gTC_2/C_1$ is a distribution coefficient that characterizes the solubility of gases in liquids, H is Henry's constant (see Seinfeld and Pandis 2006, p. 288), and R_g is the universal gas constant. The equations of convective diffusion (2) describe variations in concentration near the gas–droplet interface inside and outside the droplet

in a boundary layer approximation. The characteristic values of the Peclet number of the droplet in this study were on the order of 10^4 and 10^2 for the liquid and gaseous phases, respectively (see section 4). Consequently, the use of the boundary layer approximation is justified. The solution of Eq. (2) can be obtained using a similarity transformation pioneered by Ruckenstein (1967).

3. Method of solution

Because the boundary conditions (3) and (4) to Eq. (2) are functions of time, the solution can be found by combining the similarity transformation method with Duhamel's theorem. Equation (2) is solved by assuming first that the concentration of the absorbate in the bulk of the liquid phase in Eqs. (3) and (4) is constant. Let us introduce the following self-similar variables (see Ruckenstein 1967):

$$\eta_i = \frac{y}{\delta_i(t,\theta)} = \frac{Y}{\Delta_i}. \tag{7}$$

The variables η_i allow us to transform a system of partial differential equations (2) into a system of ordinary differential equations:

$$\frac{d^2X_i}{d\eta_i^2} + 2\eta_i \frac{dX_i}{d\eta_i} = 0, \tag{8}$$

where

$$\Delta_i^2 = \frac{4}{\mathrm{Pe}_i \sin^4\theta}\left(\cos\theta - \frac{1}{3}\cos^3\theta - \left\{\frac{1-f(\theta,T)}{1+f(\theta,T)} - \frac{1}{3}\left[\frac{1-f(\theta,T)}{1+f(\theta,T)}\right]^3\right\}\right), \tag{9}$$

$f(\theta, T) = \tan^2(\theta/2)\exp(2T)$, and $T = \mathrm{Pe}_i\tau_i = tUk/R$ is a dimensionless time. The boundary conditions to Eq. (8) are

$$X_2 = X_{b2}(T) \quad \text{as} \quad \eta_2 \to \infty, \tag{10}$$

$$X_1 = X_{b1}(T) \quad \text{as} \quad \eta_1 \to -\infty, \tag{11}$$

$$X_1 = mX_2 \quad \text{at} \quad \eta_1 = \eta_2 = 0, \quad \text{and} \tag{12}$$

$$N_1 = N_2 \quad \text{at} \quad \eta_1 = \eta_2 = 0, \tag{13}$$

where $N_i = -D_iC_i\partial x_i/\partial y$. The solutions of Eq. (8)—$\bar{x}_i$, with constant boundary conditions at $y \to \pm\infty$—are

$$\bar{x}_1 = A_1 \,\mathrm{erf}|\eta_1| + A_2 \quad \text{and} \tag{14}$$

$$\bar{x}_2 = A_3 \,\mathrm{erf}(\eta_2) + A_4, \tag{15}$$

where A_1, A_2, A_3, and A_4 are constants of integration. Substituting Eqs. (14) and (15) into the boundary conditions (10)–(13) and assuming that x_{b1} and x_{b2} are independent of time allows us to determine the constants of integration:

$$A_1 = \frac{x_{b1} - mx_{b2}}{1+\gamma mD},$$

$$A_2 = \frac{mx_{b2} + x_{b1}\gamma mD}{1+\gamma mD},$$

$$A_3 = \frac{\gamma D(mx_{b2} - x_{b1})}{1+\gamma mD}, \quad \text{and}$$

$$A_4 = \frac{x_{b2} + x_{b1}\gamma D}{1+\gamma mD}.$$

Applying Duhamel's theorem to Eqs. (14) and (15) yields a solution of Eq. (2) with time-dependent boundary conditions at infinity:

$$x_1(Y,\theta,T) = \frac{\partial}{\partial T}\int_0^T \left\{x_{b1}(\lambda) - \frac{x_{b1}(\lambda) - mx_{b2}(\lambda)}{1+m\gamma D}\,\mathrm{erfc}\left[\frac{Y}{\Delta_1(\theta, T-\lambda)}\right]\right\}d\lambda \quad \text{and} \tag{16}$$

$$x_2(Y,\theta,T) = \frac{\partial}{\partial T}\int_0^T \left\{x_{b2}(\lambda) + \frac{[x_{b1}(\lambda) - mx_{b2}(\lambda)]\gamma D}{1+m\gamma D}\,\mathrm{erfc}\left[\frac{Y}{\Delta_2(\theta, T-\lambda)}\right]\right\}d\lambda. \tag{17}$$

The variable x_{b1} is the unknown function of time, which can be determined by means of an integral material balance over the droplet (see Uribe-Ramirez and Korchinsky 2000):

$$-VC_1 \frac{dx_{b1}}{dt} = 2\pi R^2 \int_0^{\pi} N_1|_{Y=0} \sin\theta \, d\theta. \tag{18}$$

Substituting the expression for the absorbate concentration in the droplet [Eq. (16)] into Eq. (18) yields

$$X_{b1}(T) = 1 + \frac{3}{\mathrm{Pe}_1\sqrt{\pi}(1+m\gamma D)} \int_0^T [X_{b1}(\lambda) - mX_{b2}(\lambda)] \int_0^{\pi} \frac{\sin\theta}{\Delta_1(\theta, T-\lambda)} \, d\lambda, \tag{19}$$

where $\mathrm{Pe}_1 = UkR/D_1$.

Equation (19) is a linear-convolution Volterra integral equation of the second kind (Apelblat 2008, chapter 3). For the linear vertical distribution of absorbate in the atmosphere,

$$x_{b2} = x_{b20} + \mathrm{grad}\, x_{b2} \cdot z, \tag{20}$$

where x_{b200} is the concentration of an absorbate at the ground, x_{b20} is the concentration of an absorbate at the height H from the ground, z is directed from the cloud to the ground, $\mathrm{grad}\, x_{b2} = (x_{b200} - x_{b20})/H$, and $z = Ut$. Because the droplet falls with a constant velocity U, Eqs. (19) and (20) yield the following integral equation:

$$X_{b1}(T) = 1 + \frac{3}{\mathrm{Pe}_1\sqrt{\pi}(1+m\gamma D)} \times \int_0^T [X_{b1}(\lambda) - B\lambda] \int_0^{\pi} \frac{\sin\theta \, d\theta}{\Delta_1(\theta, T-\lambda)} \, d\lambda, \tag{21}$$

where $B = m(x_{200} - x_{20})R/(x_{10} - mx_{b20})kH$. Equation (19) can be written in the following form:

$$f(T) = \int_0^T f(\lambda)K(T, \lambda)d\lambda + g(T). \tag{22}$$

The method of solution of the integral [Eq. (22)] is based on the approximate calculation of a definite integral using some quadrature formula:

$$\int_a^b F(\xi)\, d\xi = \sum_{i=1}^{N} \alpha_i F(\xi_i) + R_N[F],$$

where $\xi_i \in [a, b]$, $i = 1, 2, \ldots, N$; α_i are coefficients which are independent of the function F; $R_N[F]$ is the remainder of the series after the Nth term.

Using a uniform mesh with an increment h ($T_i = T_0 + ih$, $h \equiv (T_N - T_0)/N$) and applying the trapezoidal integration rule, Eq. (22) can be reduced to a system of linear algebraic equations with a triangular matrix:

$$f(0) = g(0),$$
$$\left(1 - \frac{1}{2}hK_{ii}\right) f_i = h\left(\frac{1}{2}K_{i0}f_0 + \sum_{j=1}^{i-1} K_{ij}f_j\right) + g_i, \tag{23}$$

where $i = 1, \ldots, N$; $f_i = f(ih)$; $g_i = g(ih)$; and $K_{ij} = K(ih, jh)$. To solve the system of (23) it is required to calculate $N^2/2$ values of the kernel K_{ij}. Because $K(T, \lambda) = K(T - \lambda)$, $K_{ij} = K[(i-j)h]$ and consequently $K_{i+1j} = K[(i+1-j)h] = K\{[i-(j-1)]h\} = K_{ij-1}$. Therefore, at each time step i it is necessary to calculate only one value of the kernel K_{i0} because all other values were already determined: $K_{i1} = K_{i-1,0}$ and $K_{i2} = K_{i-1,1}$.

4. Results and discussion

Calculations of concentrations of the dissolved gas inside water droplets were performed for the droplets with a diameter of 1 mm falling in a gaseous atmosphere.

Results of the numerical solution of Eq. (21) with a linear altitude distribution of concentration of carbon dioxide in a gaseous phase for negligibly small initial concentration of the dissolved gas in a droplet are shown in Fig. 2. In the calculations it was assumed that the coefficient of diffusion of CO_2 in water is $D_1 = 1.77 \times 10^{-9}\,\mathrm{m^2\,s^{-1}}$ and in air is $D_2 = 1.42 \times 10^{-5}\,\mathrm{m^2\,s^{-1}}$, that the distribution coefficient m for CO_2 absorption in water is equal to 1.69×10^{-3}, and that the Peclet number for a 1-mm falling droplet is $\mathrm{Pe}_1 = 4.52 \times 10^4$.

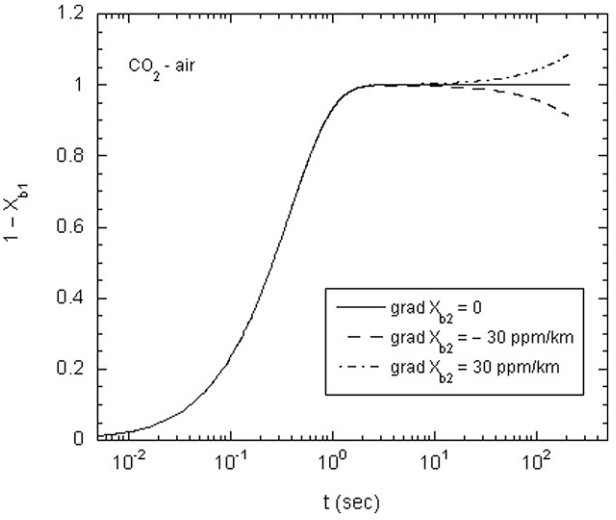

FIG. 2. Dependence of the concentration of the dissolved gas in the bulk of a water droplet vs time for absorption of CO_2 by water in the atmosphere (average concentration of CO_2 in the atmosphere is 300 ppm); $x_{b10} = 0$.

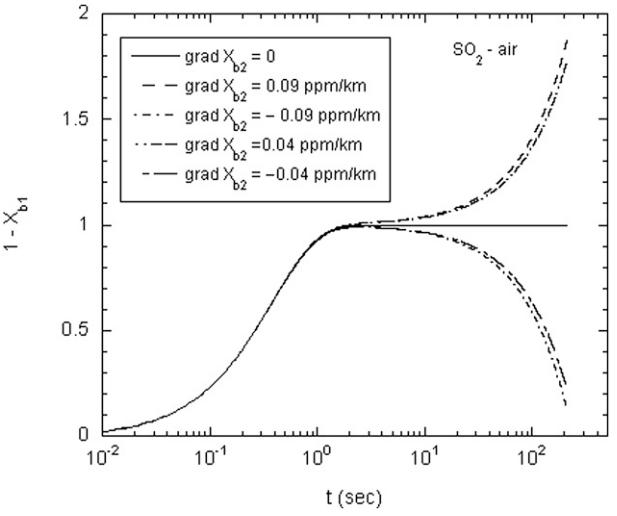

FIG. 3. Dependence of the concentration of the dissolved gas in the bulk of a water droplet vs time for absorption of SO_2 by water in the atmosphere; $x_{b10} = 0$.

We compared the results obtained using the model of gas absorption in the case of uniform distribution of soluble gases in a gaseous phase with those obtained when concentration of soluble gases varies with altitude. The comparison showed that vertical distribution of absorbate concentration in the atmospheric boundary layer (Fig. 2) strongly affects mass transfer during gas absorption by falling liquid droplets. When concentration of the absorbate is constant, the absorbate concentration in the droplet attains saturation after a certain time interval; at the final stage of their fall, droplets do not absorb soluble trace gases (see Fig. 2). In the calculations it is assumed that concentration of the absorbate in a gaseous phase in the case with a constant concentration of absorbate is equal to the height-averaged value of the concentration.

When concentration of the absorbate in the gaseous phase decreases with altitude, droplets absorb soluble gas throughout their entire fall. Consequently, concentration of the soluble gas inside droplets at the ground increases in comparison with a case when distribution of absorbate in a gaseous phase is uniform.

When concentration of the soluble gas increases with altitude, after some time droplets begin to release the dissolved gas. Consequently, beginning at some altitude gas absorption is replaced by gas desorption; therefore, concentration of the soluble gas inside droplets at the ground decreases (see Figs. 2 and 3). Results of numerical calculations of gas absorption of SO_2 by rain droplets falling in the atmosphere with a linear altitude distribution of concentration of SO_2 in a gaseous phase are presented in Fig. 3. Calculations are performed for negligibly small initial concentration of the dissolved gas in the droplet and for values of the concentration gradient in the atmosphere $|\text{grad}\, x_{b2}|$, equal to 0.09 and 0.04 ppm km^{-1}, respectively. Values of concentration of SO_2 in a cloud and at a ground were taken to be equal to 0.1, 0.01, and 0.05 ppm. The coefficient of diffusion of SO_2 in water and in air were assumed to be $D_1 = 1.67 \times 10^{-9}$ m^2 s^{-1} and $D_2 = 1.22 \times 10^{-5}$ m^2 s^{-1}, respectively; the distribution coefficient m for SO_2 absorption in water is 2.85×10^{-2}, and the Peclet number for a 1-mm-diameter droplet absorbing SO_2 is equal to $Pe_1 = 4.79 \times 10^4$. Similar to the case of CO_2 absorption, droplets absorb sulfur dioxide during their entire fall period when concentration of SO_2 in the gaseous phase decreases with altitude. When concentration of sulfur dioxide increases with altitude, after some time droplets begin to release the dissolved gas. As can be seen from Fig. 3, the increase of the concentration gradient enhances the rate of absorption/desorption by the rain droplets in the atmosphere.

Results of numerical calculations of mass transfer between the falling droplet, initially saturated up to the concentration mx_{b20}, and a surrounding gaseous atmosphere are shown in Fig. 4. If concentration of the absorbate in a gaseous phase is homogeneous and equal to x_{b20}, mass transfer between the droplet and gaseous phase during the entire droplet fall period is negligibly small. When concentration of the soluble gas in the gaseous phase decreases with altitude, droplets absorb soluble gas throughout the fall period. If concentration of the soluble trace gases in the gaseous phase increases

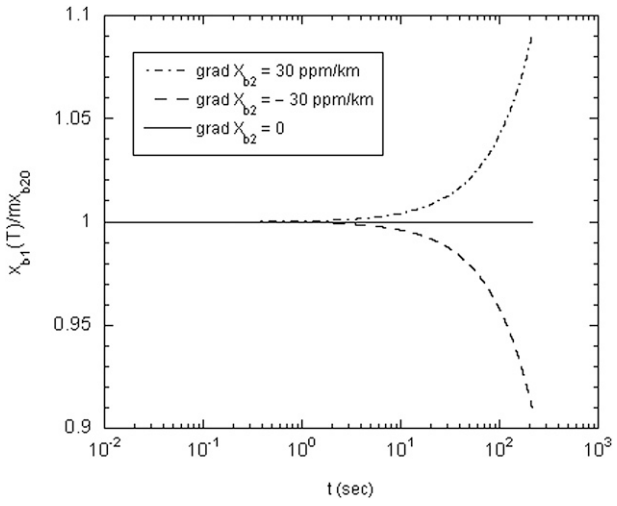

FIG. 4. Dependence of the concentration of the dissolved gas in the bulk of a water droplet vs time for absorption of CO_2 by water in the atmosphere (average concentration of CO_2 in the atmosphere is 300 ppm); $x_{b10} = mx_{b20}$.

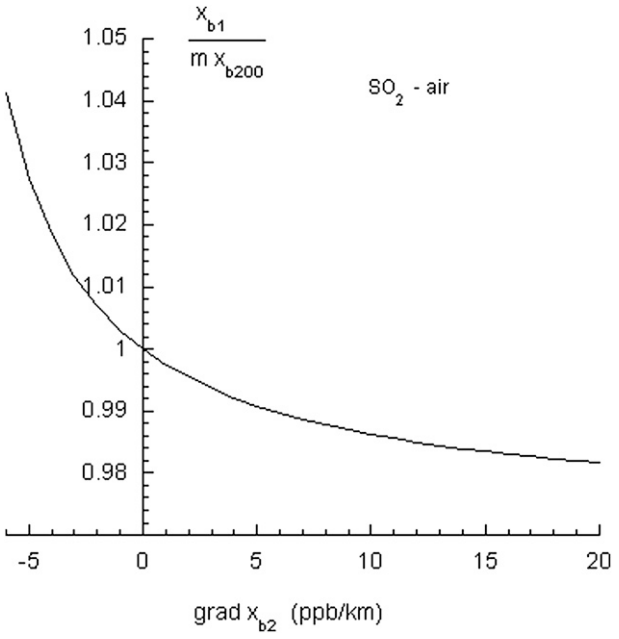

FIG. 5. Dependence of the relative concentration of the dissolved gas x_{b1}/mx_{b200} at ground vs gradx_{b2} for absorption of SO_2 by water droplet; $x_{b10} = 0$, $x_{b20} = 0.01$ ppm.

with altitude, droplets desorb soluble gas throughout their fall.

Analysis of Eq. (21) shows that the gradient of the absorbate concentration in a gaseous phase appears as a source term in the right-hand side of the Volterra equation of the second kind, which determines the dimensionless concentration of the dissolved gas inside the droplet. Consequently, the difference in the dissolved gas concentration inside the droplet for the cases with and without the source term becomes pronounced at the same time for negative and positive gradients of the absorbate concentration in the gaseous phase (Figs. 2–4).

The influence of the gradient of SO_2 in a gaseous phase on the dimensionless concentration of the dissolved gas in a droplet, x_{b1}/mx_{b200}, at the ground ($z = H$) was analyzed using the numerical solution of Eq. (21). The results of calculations are presented in Fig. 5. Concentration of the trace gas in a cloud was assumed to be constant and concentrations at the ground and in the atmosphere depend on a value of gradx_{b2}. Inspection of Fig. 5 shows that when grad$x_{b2} > 0$ and concentration of the trace gas in a gaseous phase have a maximum at the ground, $x_{b1}/mx_{b200} < 1$ at the ground. The latter implies that concentration of the dissolved gas in a droplet is lower than concentration of saturation in liquid, corresponding to x_{b200}. On the contrary, when grad$x_{b2} < 0$, $x_{b1}/mx_{b200} > 1$ at the ground and concentration of the dissolved gas in a droplet is higher than concentration of saturation in a liquid, mx_{b200}.

The influence of diurnal variations of CO_2 distribution with altitude on trace gas scavenging by a falling droplet is shown in Figs. 6 and 7. Vertical profiles of CO_2 measured by Pérez-Landa et al. (2007) at heights between 25 and 800 m at 0623 and 1303 local time during the growing season over a rice paddy field in the Valencia coastal region in Spain are approximated by logarithmic and linear functions using the least squares method (see Fig. 6). Inspection of Fig. 7 shows that changing the vertical profiles of CO_2 from logarithmic early in the morning to uniform in the afternoon (under the influence of photosynthesis and thermally driven buoyant mixing) changes the scenario of the trace gas absorption by a falling rain droplet. Early in the morning, the concentration of absorbate in the gaseous phase has a pronounced maximum at the surface and decreases with altitude. Correspondingly, the droplets absorb the soluble gas during the entire period of a free fall from a cloud to the ground.

In the afternoon, because of CO_2 vertical rectification in the atmosphere, absorbate concentration in the droplet attains saturation after a few seconds, and at the final stage of their fall droplets do not absorb soluble trace gases (see Fig. 7).

5. Summary and conclusions

In this study we considered conjugate mass transfer during soluble gas absorption by a falling droplet with the internal circulation from a mixture containing an inert gas using approximation of a thin concentration

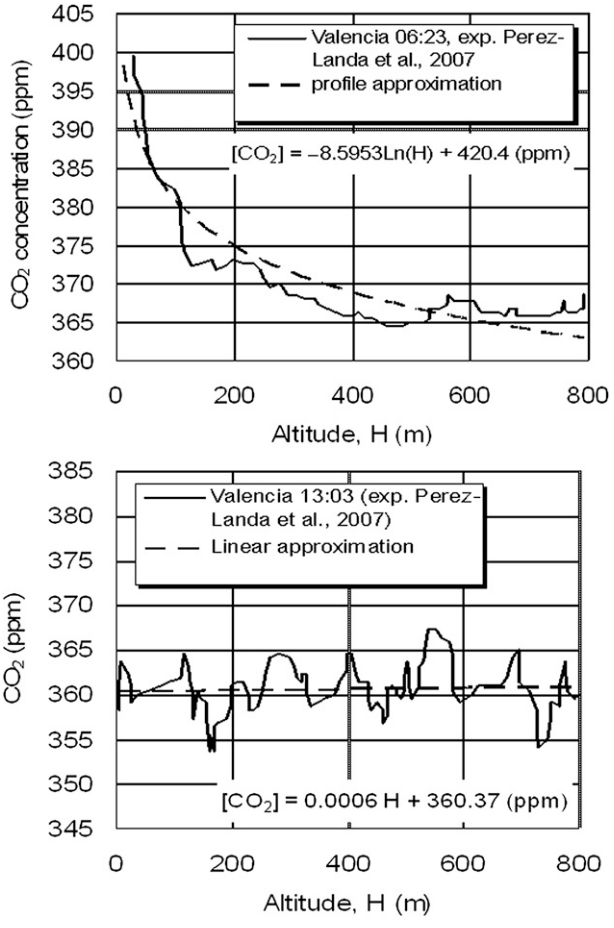

FIG. 6. Dependence of CO_2 concentration in the atmosphere on altitude in (a) morning and (b) afternoon.

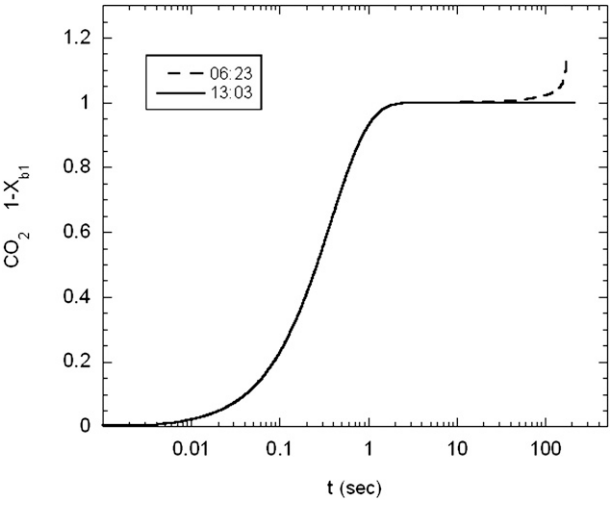

FIG. 7. Dependence of the concentration of the dissolved gas on the bulk of a water droplet vs time for absorption of CO_2 by water in the atmosphere; $x_{b10} = 0$.

boundary layer in the liquid and gaseous phases and accounting for the absorbate accumulation in the bulk of the liquid. The bulk of the droplet, beyond the diffusion boundary layer, is completely mixed and concentration of absorbate is homogeneous and time-dependent in the bulk. The system of transient partial parabolic differential equations of convective diffusion in liquid and gaseous phases with time-dependent boundary conditions has been solved by combining the similarity transformation method with Duhamel's theorem. The simple form of the obtained solutions allows us to use them in the analysis of the dependence of the rate of mass transfer on different parameters (e.g., on the radius of the droplet, diffusion coefficient, gradient of the absorbate concentration in a gaseous phase, etc.). The obtained solution can be also used for validating modeling procedures for solving more involved problems of gas absorption by falling liquid droplets.

The results obtained in this study can be summarized as follows:

1) The suggested model of gas absorption by a falling liquid droplet in the presence of inert admixtures takes into account a number of effects that were neglected in the previous studies, such as the effect of dissolved gas accumulation inside a droplet and effect of the absorbate inhomogeneity in a gaseous phase on the rate of mass transfer.
2) It is shown that the dependence of the radius-averaged concentration versus time in a falling droplet is determined by a linear-convolution Volterra integral equation of the second kind, which is easier to solve numerically than the original system of partial differential equations.
3) Vertical inhomogeneity of the soluble trace gas concentration in the gaseous phase strongly affects mass transfer during gas absorption by a falling liquid droplet. When concentration of the soluble trace gases in the atmosphere decreases with altitude, droplets absorb trace gases during their entire fall. When concentration of the soluble trace gases increases with altitude, at some altitude gas absorption begins to be replaced by gas desorption.
4) Concentration of the dissolved gas in a droplet at the ground is independent of the initial concentration of the dissolved gas in a droplet.
5) It is demonstrated that the increase of the concentration gradient of absorbate in a gaseous phase enhances the rate of gas absorption/desorption by a rain droplet in the atmosphere.
6) It is shown that when concentration of the trace gas in a gaseous phase has a maximum at the ground, concentration of the dissolved gas in a droplet at the ground is lower than concentration of saturation in a

liquid, mx_{b200}. On the contrary, when concentration of the trace gas in a gaseous phase has a minimum at the ground, the concentration of the dissolved gas in a droplet at the ground is higher than the concentration of saturation in a liquid, mx_{b200}.

The developed model can be used for the analysis of scavenging of hazardous gases in the atmosphere by rain droplets and can be incorporated into computer codes.

APPENDIX

Symbol Definitions

C_i (mol m^{-3}) = molar density at the bulk of fluid
D_i (m^2 s^{-1}) = molecular diffusion coefficient
D = square root of the diffusivities ratio $\sqrt{D_1/D_2}$
H (mol L^{-1} atm^{-1}) = Henry's law constant
k = coefficient in Eq. (1)
$N_i = -D_i C_i(\partial x_i/\partial y)$ (mol m^{-2} s^{-1}) = molar flux density
m = distribution coefficient
$\mathrm{Pe}_i = kRU/D_i$ = Peclet number for a moving droplet
r (m) = radial coordinate
R (m) = droplet radius
$\mathrm{Re} = 2URp_2/\mu_2$ = external flow Reynolds number for a moving droplet
$\mathrm{Sc} = \nu_i/D_i$ = Schmidt number
t (s) = time
$T = tUk/R$ = dimensionless time
U (m s^{-1}) = translational velocity of a droplet
v_r, v_θ (m s^{-1}) = velocity components
V (m^3) = droplet volume
x = molar fraction of an absorbate
x_{b10} = initial value of molar fraction of absorbate in a droplet
x_{b20} = value of molar fraction of an absorbate in a gas phase at height H
x_{b200} = value of molar fraction of absorbate in a gas phase on the ground
$x_{b1}(t)$ = molar fraction of absorbate in a bulk of a droplet
$x_{b2}(t)$ = molar fraction of an absorbate in a bulk of a gas phase
$X_1 = (x_1 - mx_{b20})/(x_{b10} - mx_{b20})$ = dimensionless molar fraction of absorbate in the liquid phase
$X_2 = (x_2 - x_{b20})/(x_{b10} - mx_{b20})$ = dimensionless molar fraction of an absorbate in the gaseous phase
$X_{b1}(t) = (x_{b1}(t) - mx_{b20})/(x_{b10} - mx_{b20})$ dimensionless molar fraction of an absorbate in the bulk of a droplet
$X_{b2}(t) = (x_{b2}(t) - x_{b20})/(x_{b10} - mx_{b20})$ = dimensionless molar fraction of an absorbate in the bulk of a gas phase
y (m) = distance from the surface of a droplet
$Y = y/R$ = dimensionless distance from the surface of a droplet
z (m) = coordinate in a vertical direction
$\gamma = C_1/C_2$ = molar densities ratio
δ_i (m) = thickness of a diffusion boundary layer
$\Delta_i = \delta_i/R$ = dimensionless thickness of a diffusion boundary layer
λ = variable, Eqs. (16) and (17)
η_i = similarity variable, Eq. (7)
θ (rad) = angle
μ_i (kg m^{-1} s^{-1}) = dynamic viscosity of a fluid
ν_i (m^2 s^{-1}) = kinematic viscosity of a fluid
ρ_i (kg m^{-3}) = density at the bulk of fluid
$\tau_i = tD_i/R^2$ = dimensionless time

Subscripts

0 = value on the height H in the atmosphere
1 = liquid phase
2 = gaseous phase
b = value in the bulk
r = radial direction
θ = tangential direction

REFERENCES

Alexandrova, S., M. Marion, E. Lepinasse, and A. Saboni, 2004: Mass transfer modeling of SO_2 into large drops. *Chem. Eng. Technol.,* **27,** 676–680.

Altwicker, E. R., and C. E. Lindhjem, 1988: Absorption of gases into drops. *AIChE J.,* **34,** 329–332.

Amokrane, H., and B. Caussade, 1999: Gas absorption into a moving spheroidal water drop. *J. Atmos. Sci.,* **56,** 1808–1829.

Apelblat, A., 2008: *Volterra Functions*. Nova Science, 360 pp.

Bartels, R. C. F., and R. V. Churchill, 1942: Resolution of boundary problems by the use of generalized convolution. *Bull. Amer. Math. Soc.,* **48,** 276–282.

Chen, B., J. M. Chen, J. Liu, D. Chan, K. Higuchi, and A. Shashkov, 2004: A vertical diffusion scheme to estimate the atmospheric rectifier effect. *J. Geophys. Res.,* **109,** D04306, doi:10.1029/2003JD003925.

——, ——, and D. E. J. Worthy, 2005: Interannual variability in the atmospheric CO_2 rectification over a boreal forest region. *J. Geophys. Res.,* **110,** D16301, doi:10.1029/2004JD005546.

——, ——, G. Mo, T. A. Black, and D. E. J. Worthy, 2008: Comparison of regional carbon flux estimates from CO_2 concentration measurements and remote sensing based footprint integration. *Global Biogeochem. Cycles,* **22,** GB2012, doi:10.1029/2007GB003024.

Chen, W.-H., 2001: Dynamics of sulfur dioxide absorption in a raindrop falling at terminal velocity. *Atmos. Environ.,* **35,** 4777–4790.

——, 2004: Atmospheric ammonia scavenging mechanism around a liquid droplet in convective flow. *Atmos. Environ.,* **38,** 1107–1116.

de Arellano, J. V.-G., B. Gioli, F. Miglietta, H. J. J. Jonker, H. K. Baltink, R. W. A. Hutjes, and A. A. M. Holtslag, 2004: Entrainment process of carbon dioxide in the atmospheric

boundary layer. *J. Geophys. Res.,* **109,** D18110, doi:10.1029/2004JD004725.

Denning, A. S., I. Y. Fung, and D. Randall, 1995: Latitudinal gradient of atmospheric CO_2 due to seasonal exchange with land biota. *Nature,* **376,** 240–243.

Elperin, T., and A. Fominykh, 2005: Conjugate mass transfer during gas absorption by falling liquid droplet with internal circulation. *Atmos. Environ.,* **39,** 4575–4582.

——, ——, and B. Krasovitov, 2007: Evaporation and condensation of large droplets in the presence of inert admixtures containing soluble gas. *J. Atmos. Sci.,* **64,** 983–995.

——, ——, and ——, 2008: Scavenging of soluble gases by evaporating and growing cloud droplets in the presence of aqueous-phase dissociation reaction. *Atmos. Environ.,* **42,** 3076–3086.

Georgii, H. W., 1978: Large scale spatial and temporal distribution of sulfur compounds. *Atmos. Environ.,* **12,** 681–690.

——, and W. J. Müller, 1974: On the distribution of ammonia in the middle and lower troposphere. *Tellus,* **26,** 180–184.

Gravenhorst, G., Th. Janssen-Schmidt, D. H. Ehhalt, and E. P. Röth, 1978: The influence of clouds and rain on the vertical distribution of sulfur dioxide in a one-dimensional steady-state model. *Atmos. Environ.,* **12,** 691–698.

Kaji, R., Y. Hishinuma, and H. Kuroda, 1985: SO_2 absorption by water droplets. *J. Chem. Eng. Japan,* **18,** 169–172.

Pérez-Landa, G., and Coauthors, 2007: Mesoscale circulations over complex terrain in the Valencia coastal region, Spain—Part 2: Modeling CO_2 transport using idealized surface fluxes. *Atmos. Chem. Phys.,* **7,** 1851–1868.

Pruppacher, H. R., and J. D. Klett, 1997: *Microphysics of Clouds and Precipitation*. 2nd ed. Kluwer Academic, 955 pp.

Ruckenstein, E., 1967: Mass transfer between a single drop and a continuous phase. *Int. J. Heat Mass Transf.,* **10,** 1785–1792.

Saboni, A., and S. Alexandrova, 2001: Sulfur dioxide absorption and desorption by water drops. *Chem. Eng. J.,* **84,** 577–580.

Schulz, K., M. L. Jensen, B. B. Balsley, K. Davis, and J. W. Birks, 2004: Tedlar bag sampling technique for vertical profiling of carbon dioxide through the atmospheric boundary layer with high precision and accuracy. *Environ. Sci. Technol.,* **38,** 3683–3688.

Seinfeld, J. H., and S. N. Pandis, 2006: *Atmospheric Chemistry and Physics: From Air Pollution to Climate Change*. 2nd ed. Wiley, 1225 pp.

Uribe-Ramirez, A. R., and W. J. Korchinsky, 2000: Fundamental theory for prediction of single-component mass transfer in liquid drops at intermediate Reynolds numbers ($10 \leq Re \leq 250$). *Chem. Eng. Sci.,* **55,** 3305–3318.

Walcek, C. J., and H. R. Pruppacher, 1984: On the scavenging of SO_2 by cloud and raindrops: I. A theoretical study of SO_2 absorption and desorption for water drops in air. *J. Atmos. Chem.,* **1,** 269–289.

Waltrop, A., S. K. Mitra, A. I. Flossmann, and H. R. Pruppacher, 1991: On the scavenging of SO_2 by cloud and rain drops. 4. A wind tunnel and theoretical study of the absorption of SO_2 in the ppb(v) range by water drops in the presence of H_2O_2. *J. Atmos. Chem.,* **12,** 1–17.